

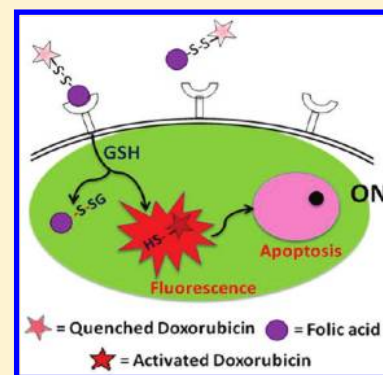
# Cell-Specific, Activatable, and Theranostic Prodrug for Dual-Targeted Cancer Imaging and Therapy

Santimukul Santra,<sup>†</sup> Charalambos Kaittaniis,<sup>†</sup> Oscar J. Santiesteban,<sup>†,§</sup> and J. Manuel Perez<sup>\*,†,§,‡</sup>

<sup>†</sup>NanoScience Technology Center, <sup>‡</sup>Burnett School of Biomedical Sciences, College of Medicine, and <sup>§</sup>Department of Chemistry, University of Central Florida, 12424 Research Parkway, Suite 400, Orlando, Florida 32816, United States

**S** Supporting Information

**ABSTRACT:** Herein we describe the design and synthesis of a folate–doxorubicin conjugate with activatable fluorescence and activatable cytotoxicity. In this study we discovered that the cytotoxicity and fluorescence of doxorubicin are quenched (OFF) when covalently linked with folic acid. Most importantly, when the conjugate is designed with a disulfide bond linking the targeting folate unit and the cytotoxic doxorubicin, a targeted activatable prodrug is obtained that becomes activated (ON) within the cell by glutathione-mediated dissociation and nuclear translocation, showing enhanced fluorescence and cellular toxicity. In our novel design, folic acid acted as both a targeting ligand for the folate receptor as well as a quencher for doxorubicin's fluorescence.



## INTRODUCTION

New targeted chemotherapeutic drugs that can report on the localization and activation of the drug upon selective cell internalization are being actively investigated for cancer treatment.<sup>1–6</sup> Receptor-targeted chemotherapeutics are attractive when they target a receptor that is overexpressed in tumors.<sup>7–9</sup> This will minimize systemic distribution of the drug while facilitating binding and internalization in cells that express the receptor. The folate receptor (FR) is a well-known tumor-associated receptor that is overexpressed in many tumors, including those of the breast, lung, kidney, and brain.<sup>10–13</sup> FR binds folic acid (folate) with high affinity, and various folate–drug conjugates have been developed and tested in culture cells, animal models, and human clinical trials with successful results.<sup>4,14–16</sup> Examples include folate conjugates of cytotoxic drugs, such as camptothecin,<sup>17</sup> taxol,<sup>18</sup> mitomycin C (EC 72),<sup>19–21</sup> and folate-tethered protein toxins, such as momordin<sup>22</sup> and the *Pseudomonas* exotoxin<sup>23</sup> among others. In most of these cases, the drug is conjugated via a cleavable linker, forming a prodrug that releases the active drug upon cell internalization. However, none of these conjugates possess activatable cytotoxicity or activatable fluorescence to assess drug release and intracellular localization upon cell entry.<sup>17–23</sup> On the other hand, various folate conjugates with fluorescent dyes and nanoparticles have been developed and used to interrogate the presence of the folate receptor and the final localization of the conjugate in cultured cells.<sup>24,25</sup> However, these fluorescent folate conjugates lack therapeutic modality. Therefore, a FR-targeting theranostic molecular probe with both imaging and therapeutic properties that can become activated upon selective internalization into FR expressing tumor cells could facilitate studies aimed at

investigating the mechanism of probe internalization and cytotoxicity in cultured cells.

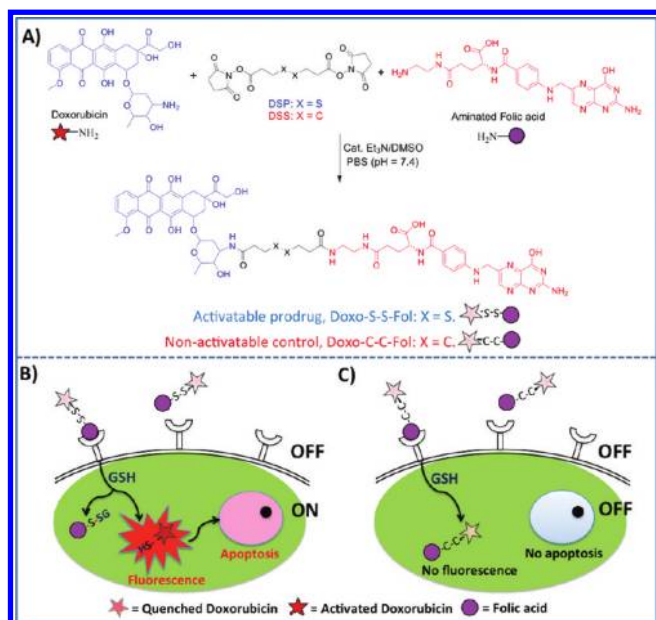
An activatable, FR-targeted theranostic agent that combines fluorescent and cytotoxic (prodrug) modalities and become activated upon cell internalization would be an attractive candidate to these studies. Typically, an activatable molecular imaging agent becomes activated upon interaction with a specific enzyme associated with disease, resulting in an increase in its signal output.<sup>4,24,26–33</sup> This capability allows for increased image resolution and lower signal background. Meanwhile, a cytotoxic prodrug is designed to be less active and therefore less toxic until it becomes metabolized inside the body within the targeted organ.<sup>34–40</sup> Herein we report a folate–doxorubicin activatable theranostic prodrug for targeted delivery to folate receptor-expressing cancer cells (Scheme 1). We discovered that both the fluorescence and cytotoxicity of doxorubicin (Doxo) are quenched (OFF) when covalently linked to folic acid (Fol). This finding indicates that folic acid can act as both a receptor-targeting ligand and a quencher for doxorubicin. The activatable theranostic prodrug was designed with a disulfide (“S–S”) linker, dithiobis(succinimidyl propionate) (DSP), between the fluorescent doxorubicin and the folic acid (Scheme 1A). Various prodrugs have been previously designed with a disulfide linker connecting folate and the corresponding drug, resulting in the generation of the active drug upon cleavage with glutathione, an intracellular reducing agent.<sup>4,17,20,21</sup>

However, none of these probes reports on an activatable fluorescent capability based on the quenching ability of the

**Received:** August 8, 2011

**Published:** September 12, 2011

### Scheme 1. Intracellular Reduced Glutathione (GSH) Activates a Targetable Theranostic Prodrug, Leading to Target-Specific Cytotoxicity and Fluorescence Emission<sup>a</sup>



<sup>a</sup> (A) Syntheses of activatable Doxo-S-S-Fol prodrug and nonactivatable control Doxo-C-C-Fol probe. (B) Once in the extracellular milieu, fluorescence emission and cytotoxicity of the prodrug (Doxo-S-S-Fol) are quenched (OFF). Upon target-specific internalization, enhanced fluorescence emission and cytotoxicity (ON) occurs due to cleavage of the disulfide bond. (C) The noncleavable control Doxo-C-C-Fol probe, although it undergoes internalization, remains biologically inactive (OFF) with quenched fluorescence, due to the absence of a cleaving mechanism.

targeting ligand (Fol) toward the fluorescent drug (Doxo). We hypothesized that upon internalization into FR-expressing cancer cells, our activatable FR-targeted theranostic agent will become activated (ON) in the presence of intracellular reduced glutathione (GSH), leading to increased fluorescence and cytotoxicity (Scheme 1B). In contrast, it will remain in an OFF state outside the cell, where the GSH levels are low, or when the Doxo is covalently attached to folic acid (Doxo-C-C-Fol) using a more stable linker, disuccinimidyl suberate (DSS, spacer arm 11.4 Å) with alkane bonds (“C-C”) (Scheme 1C). Results showed that the newly developed Doxo-S-S-Fol theranostic probe becomes selectively activated upon internalization into FR expressing cells, becoming fluorescent and cytotoxic. The fluorescent capability of the activated probe allowed us to monitor the probe’s intracellular localization and eventual migration to the nucleus, before becoming cytotoxic. Therefore, our newly developed folate-targeting theranostic prodrug (Doxo-S-S-Fol) combines features of several important modalities, such as, (i) receptor-targeted internalization, (ii) activatable fluorescence emission, (iii) activatable cytotoxicity, and (iv) use of clinically approved components. These features make Doxo-S-S-Fol an excellent agent for the monitoring of the progress of cancer therapy.

## RESULTS AND DISCUSSION

The synthesis route for the activatable probe Doxo-S-S-Fol is shown in Scheme 1. First, folic acid is aminated using

ethylenediamine and carbodiimide chemistry as previously reported (Supporting Information Scheme S1).<sup>41</sup> Then, the aminated folic acid was conjugated to the amino group on doxorubicin using dithiobis(succinimidyl propionate) (DSP, spacer arm 12 Å), a cleavable disulfide linker. We decided to conjugate Doxo via its amine group instead of the ketone, as conjugation via the amine group is easier, and upon cleavage of the disulfide bond, a short thiol ligand (3-mercapto-propanone) would be still attached to Doxo. Previous reports<sup>38,42–44</sup> indicate that a low molecular weight linker attached to Doxo’s amine group does not reduce the potency of the drug.

As a control probe, a noncleavable linker disuccinimidyl suberate (DSS, spacer arm 11.4 Å) was used instead to synthesize the nonactivatable probe Doxo-C-C-Fol. The Doxo-C-C-Fol probe serves as a nonactivatable control probe with quenched fluorescence emission and cytotoxicity. These conjugates were characterized by mass spectrometry, HPLC (Supporting Information Figures S1 and S2), and UV-vis spectroscopy (Supporting Information Figure S3). UV-vis spectroscopic results showed a red shift (10 nm) in the absorption maximum of the activatable probe compared to uncoupled doxorubicin, further confirming the successful conjugation of Doxo with Fol. Both probes (5 mM) were found to be stable in PBS (pH = 7.4) and serum for days (Supporting Information Figure S4). Surprisingly, upon conjugation of doxorubicin to folic acid using either DSP or DSS linker, the fluorescence of the resulting conjugate was quenched 5-fold (Supporting Information Figure S5). To our knowledge, the quenching of doxorubicin by proximity to folic acid has never been reported. This is indeed unexpected, as the excitation wavelength of folic acid does not overlap with Doxo emission wavelength, ruling out any fluorescent energy transfer (FRET) mechanism.

To test our hypothesis, we first investigated if treatment of the prodrug with GSH resulted in fluorescence activation. In these experiments, each probe in PBS (pH = 7.4) was incubated with a GSH solution (5 mM, 1:1 molar ratio), and their fluorescence emissions ( $\lambda_{\text{ex}} = 497 \text{ nm}$ ,  $\lambda_{\text{em}} = 594 \text{ nm}$ ) were measured at different time points. We picked a GSH concentration of 5 mM, as the intracellular GSH concentration is between 1 and 10 mM, whereas in the blood, it is in the micromolar range (1–10  $\mu\text{M}$ ).<sup>45</sup> As shown in Figure 1A, the fluorescence emission of Doxo-S-S-Fol increased 5-fold (dequenched) as a result of the reduction (cleavage) of the disulfide bond, reaching a plateau within 3 h. As expected, a nominal increase in fluorescence was observed in the case of Doxo-C-C-Fol (Figure 1B). In addition, treatment of unconjugated Doxo (5 mM in PBS pH = 7.4) with GSH (5 mM in PBS pH = 7.4) shows no effect on the fluorescence emission of doxorubicin (Supporting Information Figure S6), suggesting that the observed increase in fluorescence of the Doxo-S-S-Fol probe was due to GSH-mediated cleavage of the disulfide bond. To prove the stability of our theranostic probe (1.2  $\mu\text{M}$ , in PBS pH = 7.4, 37 °C) at the micromolar concentrations of GSH present in the blood and eventual activation at millimolar concentrations inside the cell, we compared the activation of Doxo-S-S-Fol at physiologically relevant millimolar (1–10 mM) and micromolar (1–10  $\mu\text{M}$ ) concentrations. Results show that within 30 min of incubation, a concentration-dependent enhanced fluorescence was observed (Supporting Information Figure S7) when the intracellular GSH concentrations (1–10 mM) were used. In contrast, a nominal increase in fluorescence was observed in the presence of GSH’s extracellular concentrations (1–10  $\mu\text{M}$ ), further indicating the stability of the prodrug in the bloodstream and its activation only in the presence of intracellular GSH

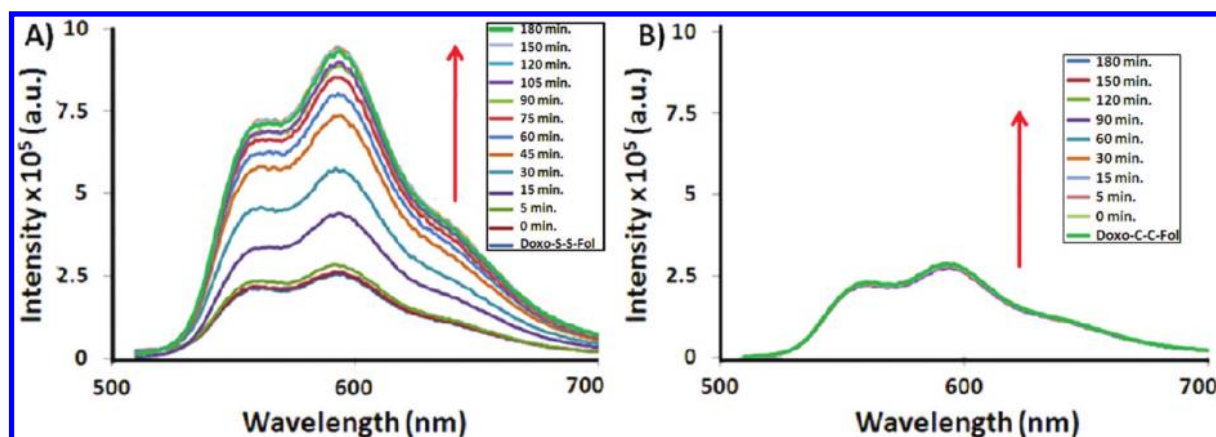


**Figure 1.** Activation of the fluorescent prodrug Doxo-S-S-Fol by GSH (5 mM) treatment. (A) Enhanced fluorescence emission ( $\lambda_{\text{ex}} = 497$  nm,  $\lambda_{\text{em}} = 594$  nm) was observed after treatment of the Doxo-S-S-Fol (5 mM) in PBS (pH = 7.4) with GSH at 37 °C. (B) The fluorescence emission of Doxo-C-C-Fol (5 mM) in PBS (pH = 7.4) does not change in the presence of GSH, leaving the prodrug in its initial quenched state.

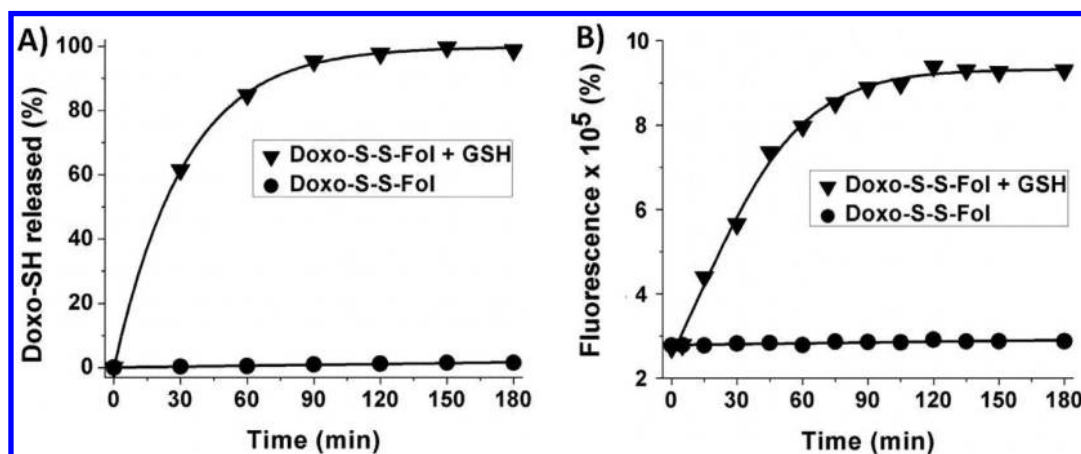


**Figure 2.** (A) Doxo-SH release from Doxo-S-S-Fol in 1.0 mL of PBS (pH = 7.4) in the presence ( $\blacktriangledown$ ) or absence ( $\bullet$ ) of GSH (1:1 molar ratio) at 37 °C. (B) Fluorescence emission ( $\lambda_{\text{ex}} = 497$  nm,  $\lambda_{\text{em}} = 594$  nm) of a Doxo-S-S-Fol solution in 1.0 mL of PBS (pH = 7.4) in the presence ( $\blacktriangledown$ ) or absence ( $\bullet$ ) of GSH (1:1 molar ratio) at 37 °C.

concentrations. Similar activation results were obtained when the probes were incubated with dithiothreitol (DTT), an alternative reducing agent for the disulfide bond (Supporting Information Figure S8). In addition, a nominal increase (1.5-fold) in fluorescence emission ( $\lambda_{\text{ex}} = 497$  nm,  $\lambda_{\text{em}} = 594$  nm) was observed after incubation of Doxo-S-S-Fol (5 mM) for up to 12 h with PBS buffer at pH = 5.0 (Supporting Information Figure S9), suggesting that the endosomal acidic microenvironment is not enough to cause activation of our probe. Taken together, these findings support the fact that folate acts as a quencher of doxorubicin and that cleavage of the disulfide bond using intracellular reducing agents, such as GSH, can restore the fluorescence of this probe.

Next, we investigated if the observed GSH-induced fluorescence activation of Doxo-S-S-Fol is due to cleavage of the disulfide linkage, with a corresponding release of the sulfhydryl-modified doxorubicin (Doxo-SH). For this study, the Doxo-S-S-Fol prodrug was incubated with GSH (1:1 molar ratio) in PBS (pH = 7.4) at 37 °C, and the reaction was monitored by HPLC chromatography to monitor the release of Doxo-SH in a timely manner. Results showed that upon incubation with GSH, a time dependent increase in the percent of Doxo-SH released was observed ( $\blacktriangledown$ , Figure 2A). The observed increase in the

amount of released Doxo-SH monitored by HPLC was accompanied by a gradual increase in fluorescence intensity recorded fluorimetrically at 594 nm ( $\blacktriangledown$ , Figure 2B). This indicated that indeed the cleavage of the disulfide probe and subsequent release of Doxo-SH results in activation of the probe and restoration of fluorescence. In contrast, a control sample without GSH treatment did not show release of Doxo-SH ( $\bullet$ , Figure 2A) and therefore did not increase in fluorescence ( $\bullet$ , Figure 2B). These results further indicated that Doxo-S-S-Fol became activated after glutathione-mediated cleavage of the disulfide linker.

In addition, the observed increase in fluorescence intensity upon cleavage further confirmed that the folic acid acted as a quencher and that the fluorescence of doxorubicin was restored upon release of Doxo-SH. After confirming the fluorescence activation of Doxo-S-S-Fol in the presence of GSH, we examined the cytotoxicity of the cleavable agent Doxo-S-S-Fol and compared it with that of the noncleavable Doxo-C-C-Fol on cells that express FR. We hypothesized that the cleavable probe will be more toxic than the noncleavable one and that the Doxo-SH that results after GSH cleavage of Doxo-S-S-Fol is as toxic as regular Doxo. For cytotoxicity experiments, we used A549 lung carcinoma cells that express the folate receptor<sup>46–49</sup>

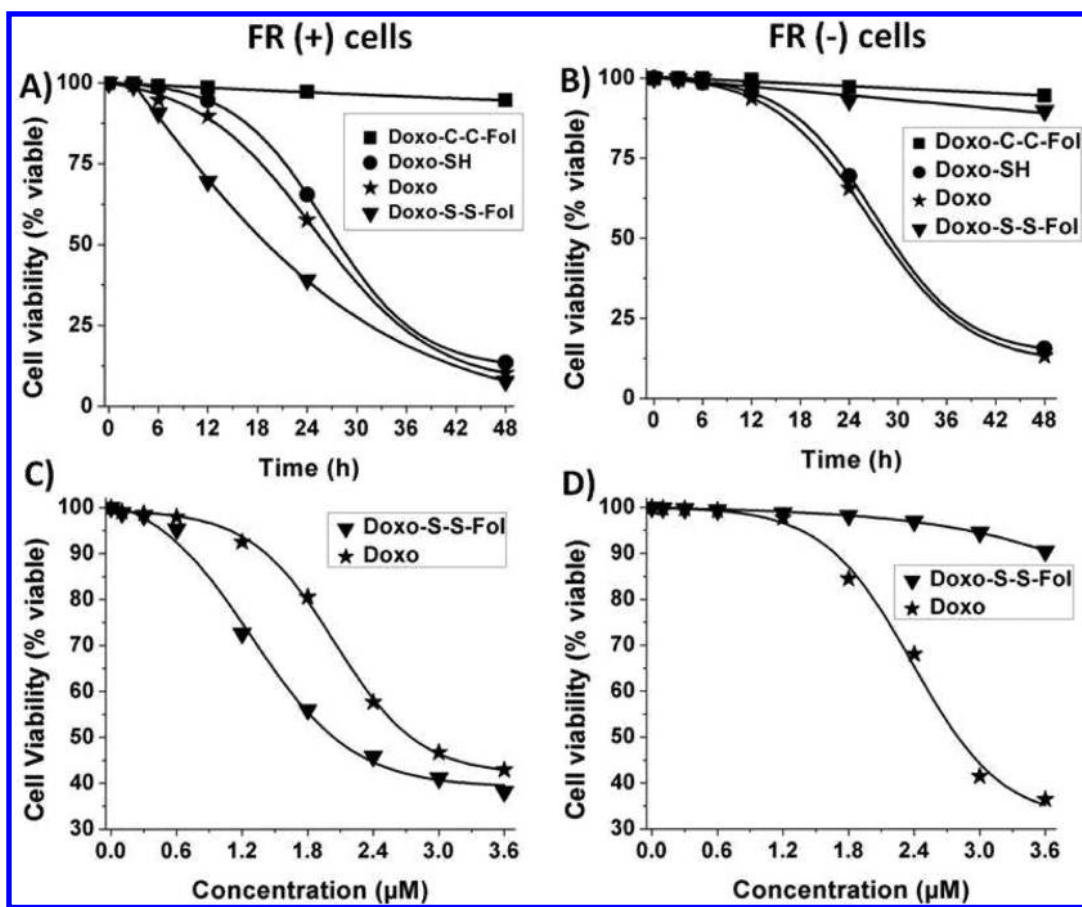


**Figure 3.** (A, B) Time-dependent and (C, D) dose-dependent viabilities of A549 cells (A, C) and MCF 7 cells (B, D) treated with synthesized prodrugs and small molecule drugs ( $1.2 \mu\text{M}$  in PBS pH = 7.4).

to compare the cytotoxicity of the activatable probe (Doxo-S-S-Fol) to the noncleavable control (Doxo-C-C-Fol), Doxo and Doxo-SH. Results showed a time-dependent decrease (Figure 3A) in the number of viable cells (2500 cells/well) upon treatment with Doxo-S-S-Fol probe ( $\blacktriangledown$ ,  $1.2 \mu\text{M}$ ). Within 48 h, almost 90% of the cells were dead when incubated with the cleavable Doxo-S-S-Fol probe as opposed to the more stable Doxo-C-C-Fol probe, which only caused 5% cell death within 48 h. When Doxo-S-S-Fol was compared to Doxo ( $\star$ ,  $1.2 \mu\text{M}$ ) or Doxo-SH ( $\bullet$ ,  $1.2 \mu\text{M}$ ), similar toxicity profiles were observed (Figure 3A) with 90% of the cells dead within 48 h. However, the targeted and activatable probe Doxo-S-S-Fol triggered faster cell death, presumably due to its folate-receptor mediated internalization as 50% of cell death occurred within the first 20 h of incubation. Meanwhile, only a 25% cell death was observed with Doxo and a slightly lower percentage (20%) with the Doxo-SH (Figure 3A). The noncleavable Doxo-C-C-Fol probe ( $\blacksquare$ ,  $1.2 \mu\text{M}$ ) exhibited no cytotoxicity upon folate receptor-mediated internalization in A549 cells (Figure 3A) as expected. In contrast, when MCF 7 breast carcinoma cell line that lack the folate receptor<sup>41,50</sup> were incubated with Doxo-S-S-Fol ( $\blacktriangledown$ ,  $1.2 \mu\text{M}$ ), minimal toxicity was observed (Figure 3B). Meanwhile, both Doxo and Doxo-SH seemed to be equally toxic in both the folate positive (A549) and folate negative (MCF 7) cells. The similar cytotoxicity profiles of both Doxo and Doxo-SH indicated that the sulfhydryl modification on Doxo did not affect doxorubicin's cytotoxicity. These findings are in agreement

with reports in the literature showing that a leucine-modified doxorubicin (Leu-Doxo)<sup>38,42</sup> ligand conjugated via doxorubicin's amine group showed comparable cytotoxicity with the free doxorubicin. This is likely due to the fact that small molecule modifications on the doxorubicin's amine group does not seem to affect its intercalation<sup>51</sup> with the cellular DNA. Overall, these findings indicated that our activatable theranostic prodrug Doxo-S-S-Fol becomes cytotoxic after FR-mediated internalizations and GSH-induced cleavage, whereas, the noncleavable control Doxo-C-C-Fol probe remains nontoxic due to the absence of any cleavage mechanisms. Both probes showed nominal cytotoxicity to FR-negative cells, confirming the receptor-mediated internalization and targeted delivery of the therapeutic drugs. In addition, as Doxo and Doxo-SH seem to internalize nonspecifically, they exhibited a slower rate of cytotoxicity toward both the cells, irrespective of the levels of FR expression when compared to Doxo-S-S-Fol.

To further compare the toxicity profiles of our activatable prodrug Doxo-S-S-Fol with free doxorubicin, dose-dependent cytotoxicity experiments were performed. In these experiments, both FR(+) and FR(-) cells were treated with different concentrations of Doxo-S-S-Fol and free Doxo for 12 h. The results confirmed the higher cytotoxicity of our Doxo-S-S-Fol probe ( $\text{IC}_{50} = 1.27 \mu\text{M}$ ) compared to Doxo ( $\text{IC}_{50} = 2.03 \mu\text{M}$ ) in FR(+) cells (Figure 3C). In contrast, Doxo-S-S-Fol probe did not show a dose-dependent cytotoxicity when FR(-) cells were used (Figure 3D). In another set

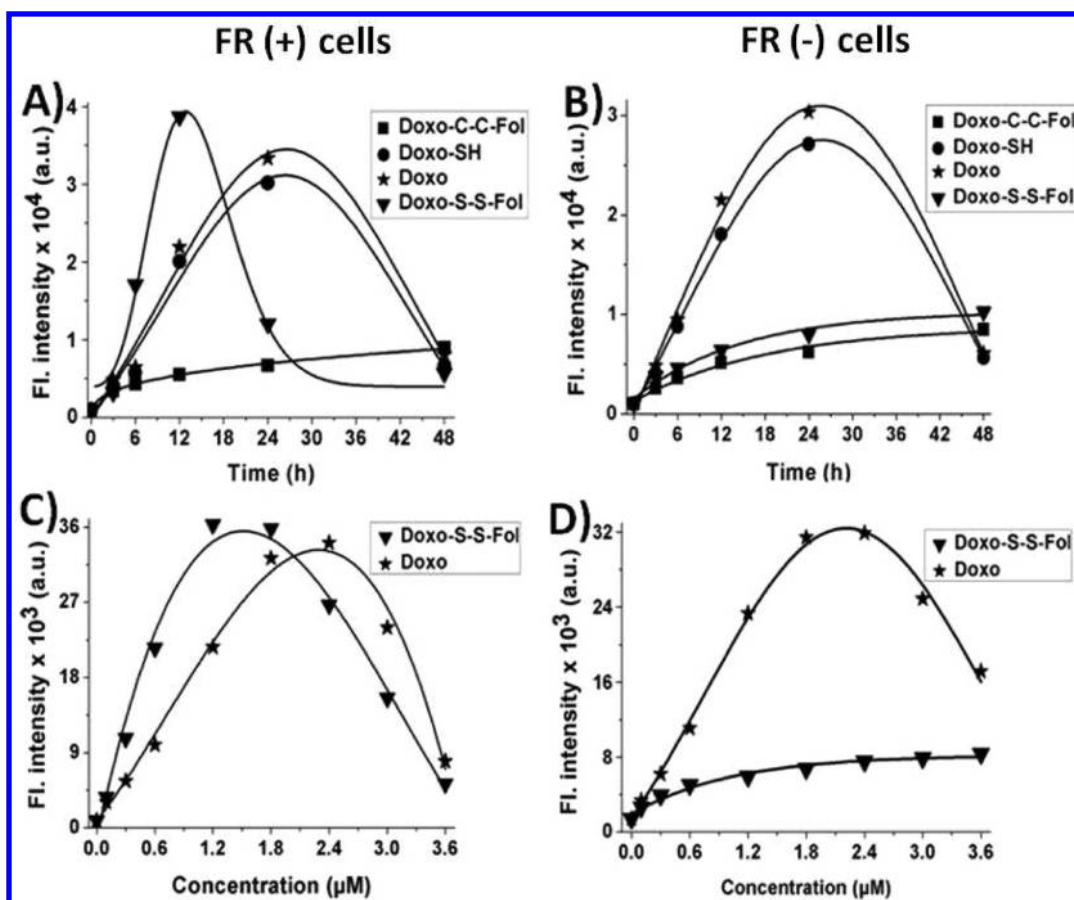


**Figure 4.** (A, B) Time-dependent and (C, D) dose-dependent intracellular fluorescence emissions from FR(+) cells (A, C) and FR(−) cells (B, D) treated with synthesized prodrugs and small molecule drugs ( $1.2 \mu\text{M}$  in PBS pH = 7.4).

of experiments, the selective cytotoxicity of Doxo-S-S-Fol to FR(+) cells was abrogated by preincubating the cells with excess free folic acid (Supporting Information Figure S10), further confirming the folate receptor-mediated internalization and selective activation of our probes. Taken together, these results indicated that the Doxo-S-S-Fol probe selectively internalizes into FR expressing cells thereby becoming highly toxic to cells that express this receptor. In contrast, Doxo is toxic irrespective of the presence or absence of FR.

To further corroborate the folate-receptor mediated internalization and subsequent fluorescence activation of Doxo-S-S-Fol and how it correlates with cytotoxicity, we investigated the rate of cell internalization and intracellular activation of the probe Doxo-S-S-Fol, compared to the noncleavable probe, Doxo-SH and Doxo (Figure 4). The FR(+) cells (2,500 cells/well) were treated with Doxo-S-S-Fol, Doxo-C-C-Fol, Doxo and Doxo-SH ( $1.2 \mu\text{M}$ ), and their fluorescence emissions were measured at different time points using a fluorescence microtiter plate reader. Results indicated a faster internalization and fluorescence activation of Doxo-S-S-Fol (▼,  $1.2 \mu\text{M}$ , Figure 4A) reaching a maximum cell-associated fluorescence intensity within 12 h. Then, the cell associated fluorescence intensity rapidly decreased after 12 h of incubation due to the selective cytotoxicity of the probe that reduces the number of viable fluorescent cells. Meanwhile, Doxo (★) and Doxo-SH (●) exhibited a much slower rate of internalization, reaching a maximum cell-associated fluorescence intensity after 24 h (Figure 4A). In contrast, FR(+) cells treated with

the noncleavable Doxo-C-C-Fol (■, Figure 4A) exhibit a minimal increase in fluorescence as expected. In FR(−) cells, however, a lower fluorescence emission was observed when treated with either activatable Doxo-S-S-Fol or nonactivatable Doxo-C-C-Fol probes (▼ and ■, Figure 4B), further confirming the need for a receptor-mediated internalization and fluorescence activation of the Doxo-S-S-Fol probe. Meanwhile, dose-dependent, cell associated fluorescence activation experiments show a fast increase in cell associated fluorescence that reached a maximum value of  $1.5 \mu\text{M}$  for Doxo-S-S-Fol (▼, Figure 4C) and  $2.5 \mu\text{M}$  for regular Doxo (★, Figure 4C) treated FR(+) cells. In contrast, when these experiments were carried out using FR(−) cells, the cell associated fluorescence for the cells treated with the Doxo-S-S-Fol was greatly reduced (▼, Figure 4D) due to the lack of a folate receptor-mediated internalization and activation of the probe. Taken together, these findings confirmed that the Doxo-S-S-Fol probe has selective cytotoxicity for folate receptor-expressing cells. In contrast, Doxo exhibits nonselective cytotoxicity, independent of the presence of the folate receptor for internalization. Furthermore, the observed rates of internalization of the various probes (Figure 4A) explain why our activatable prodrug Doxo-S-S-Fol is more cytotoxic than Doxo and Doxo-SH toward cells that express the folate receptor. The observed slow rate of fluorescence emission from Doxo and Doxo-SH treated cells, irrespective of the level of expression of the folate receptor, further confirmed their nonspecific internalizations. Yet, the significant cytotoxicity observed by Doxo-SH, the form of Doxo generated

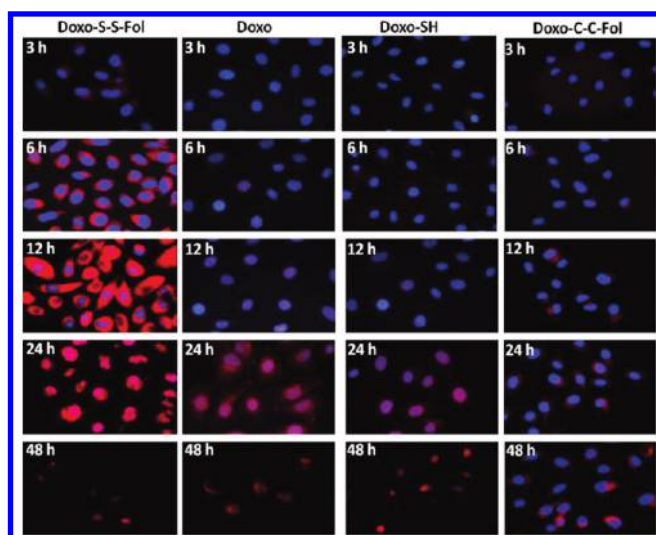


**Figure 5.** In vitro activation of a fluorescent prodrug. Left column: Fluorescence microscopy images showing internalization of the prodrug Doxo-S-S-Fol ( $1.2 \mu\text{M}$  in PBS pH = 7.4) by folate receptor-expressing A549 cells (10 000 cells) leads to enhanced fluorescence emission within 12 h and induction of apoptosis. Middle columns: Internalization of Doxo and Doxo-SH ( $1.2 \mu\text{M}$  in PBS pH = 7.4) into A549 cells shows intercalation with the nucleus within 24 h and cell death after 48 h. Right column: Minimal fluorescence emission and absence of apoptosis are observed in A549 cells treated with the control probe Doxo-C-C-Fol ( $1.2 \mu\text{M}$  in PBS pH = 7.4). Nucleus stained with DAPI (blue).

after cleavage of Doxo-S-S-Fol with GSH, verified that the sulfhydryl modification to Doxo does not diminish its cytotoxicity.

Additionally, the mechanism of action of the Doxo-S-S-Fol was studied by performing time-course fluorescence microscopy experiments using FR(+) cells (10 000 cells) treated with Doxo-S-S-Fol, Doxo, Doxo-SH, and Doxo-C-C-Fol ( $1.2 \mu\text{M}$  in PBS pH = 7.4). When the cells were treated with Doxo-S-S-Fol, a time-dependent increase in fluorescence intensity was observed in the cell cytoplasm due to internalization and intracellular GSH-induced activation of the prodrug (left column, Figure 5). The observed activation process was visible during the first 6 h and seemed to plateau within 12 h. These results were also confirmed by flow cytometry (left column, Figure 6), showing a similar time-dependent activation. At this point, the cleavage of the disulfide linkage allows for efficient migration of the resulting Doxo-SH moieties from the cytoplasm to the nucleus, where presumably they intercalate<sup>51</sup> into the cell's DNA, inducing cell death. This process was easily observed by fluorescence microscopy after 12 h of treatment, where the resulting Doxo-SH fluorescence starts to colocalize with nuclear 4',6-diamidino-2-phenylindole (DAPI) fluorescence indicating its migration to the nucleus. Dramatic changes in nuclear morphology were observed within 24 h, with a significant number of dead cells. In contrast, Doxo and Doxo-SH did not internalize as quickly as the Doxo-S-S-Fol, reaching maximum cell cytoplasm fluorescence within 24 h of incubation and induction of cell death after 48 h (middle columns, Figure 5). These results further demonstrated the slower rate of nonspecific internalization and sustained cytotoxicity of Doxo-SH, compared to Doxo. Doxo-C-C-Fol ( $1.2 \mu\text{M}$ ), however, exhibited nominal cytoplasm fluorescence and no nuclear translocation in A549 cells even after 48 h of incubation, confirming

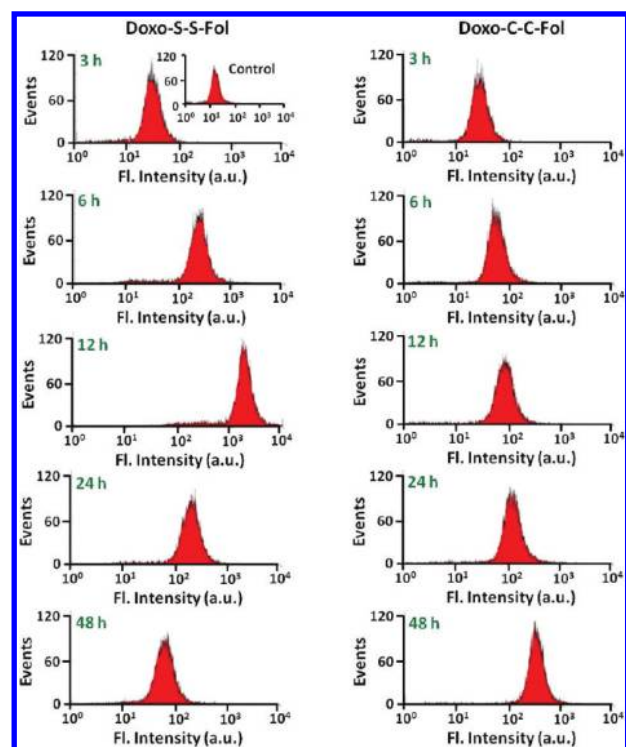


**Figure 6.** In vitro flow cytometry analysis of activation of fluorescent prodrug. Left column: Enhanced fluorescence emission due to activation and then decreased fluorescence emission due to induction of apoptosis is observed in A549 cells (10 000 cells) incubated with activatable Doxo-S-S-Fol probe ( $1.2 \mu\text{M}$  in PBS pH = 7.4). Right column: Minimal fluorescence emission and absence of apoptosis are observed in A549 cells treated with the control probe Doxo-C-C-Fol ( $1.2 \mu\text{M}$  in PBS pH = 7.4).

the lack of activation and hence migration to the nucleus of this probe (right column, Figure 5). Corresponding flow cytometry studies (right column, Figure 6) verified this observation by displaying a nominal increase in cell associated fluorescence when the Doxo-C-C-Fol probe was used. These results indicate that indeed the designed activatable probe (Doxo-S-S-Fol) behaves as a fluorescent prodrug, only becoming toxic upon folate-mediated internalization and intracellular cleavage of the disulfide bond by GSH. Furthermore, neither activation of fluorescence nor cell death were observed from the activatable Doxo-S-S-Fol prodrug when the FR(+) cells were preincubated with an excess of free folic acid, further indicating folate receptor-mediated internalizations of our probes (Supporting Information Figure S11). In other experiments, no significant cell associated fluorescence was observed when FR(-) cells were incubated with either of the probes (Supporting Information Figure S12), further confirming the folate receptor-mediated internalization and activation of the probe.

## CONCLUSION

In summary, we report a novel activatable theranostic prodrug, in which both the fluorescence and cytotoxicity of the drug (Doxo) are quenched when covalently attached to the receptor-targeting ligand (Fol). We observed that the fluorescence of doxorubicin is quenched 5-fold after binding to folic acid. The activatable probe Doxo-S-S-Fol becomes fluorescent and

cytotoxic upon receptor-mediated internalization and subsequent GSH-induced cleavage of the disulfide bond that results in the release of Doxo-SH, the active fluorescent and cytotoxic species. The presence of folate on the activatable probe guarantees a selective activation only in folate-receptor positive cells, minimizing toxicity to cells that do not express the receptor. In contrast, the noncleavable probe Doxo-C-C-Fol remains quenched showing no migration to the nucleus and therefore no toxicity. These results are in agreement with previous reports of doxorubicin prodrugs that involved attachment of peptides and biodegradable polymers to the free amino group of doxorubicin, rendering the prodrug not toxic until the peptide or biodegradable polymer is cleaved or degraded.<sup>38,42–44</sup> Our results also confirmed that the sustained cytotoxicity of the released Doxo-SH derivative is compared to free Doxo. Finally, the excellent plasma stability of the disulfide linker (half-life: 47 h in mice)<sup>46</sup> would make our activatable Doxo-S-S-Fol probe suitable in clinical settings

## MATERIALS AND METHODS

**Chemicals.** Doxorubicin (Doxo), 3-(4,5-dimethylthiazol-2-yl)-2,5-diphenyltetrazolium bromide (MTT), *N*-hydroxysuccinimide (NHS), glutathione (GSH), folic acid (Fol), isopropanol, hydrochloric acid triethylamine, and other chemicals were purchased from Sigma-Aldrich and used without further purification. Dithiobis(succinimidyl propionate) (DSP), disuccinimidyl suberate (DSS), and 1-ethyl-3-[3-dimethylaminopropyl] carbodiimide hydrochloride (EDC) were obtained from Pierce Biotechnology, whereas 4',6-diamidino-2-phenylindole (DAPI-D1306) was purchased from Invitrogen. The human lung FR(+) carcinoma cell and breast carcinoma FR(–) cell lines were obtained from ATCC. Dithiothreitol (DTT) and other chemicals were purchased from Fisher Scientific and used as received, unless otherwise stated.

**Synthesis of Activatable Prodrug Doxo-S-S-Fol.** Aminated folic acid (Supporting Information Scheme S1) was synthesized by using water-soluble carbodiimide (EDC/NHS) chemistry, as described in the previously reported method.<sup>41,52,53</sup>

Then, the aqueous solution of doxorubicin hydrochloride salt was added to PBS buffer solution (pH = 8.4) to obtain doxorubicin with a free amine group. The resulting solution was centrifuged, and the solid pellet was soluble in dimethyl sulfoxide (DMSO). In a typical reaction, to a mixture of aminated folic acid (1.84 mM in PBS, pH = 7.4) and doxorubicin (1.84 mM in DMSO) solutions, a dithiobis(succinimidyl propionate) (DSP) solution (1.84 mM in DMSO) was added dropwise. A catalytic amount of triethylamine (0.4  $\mu$ L in DMSO) was added to the reaction mixture. The progress of the reaction was monitored by TLC in 9:1 of chloroform and methanol. The reaction mixture was kept at room temperature for 30 min, before overnight incubation at 4 °C. The reaction mixture was then loaded on a silica gel column (flash column chromatography) to isolate the pure product using chloroform and methanol as eluent. The prodrug (Doxo-S-S-Fol) was kept at 4 °C as stock solutions.

The synthesized probe was characterized by electrospray ionization mass spectrometry (Waters dedicated LC/MS auto purification system) and HPLC, showing the formation of highly pure activatable probe (Supporting Information Figure S1). The yield of the prodrug Doxo-S-S-Fol was 72%. ESMS (ES + ve), (MH<sup>+</sup>)<sub>calcd</sub> for C<sub>54</sub>H<sub>61</sub>N<sub>10</sub>O<sub>18</sub>S<sub>2</sub>: 1202.49, found 1202.55.

**Synthesis of Control Prodrug Doxo-C-C-Fol.** The control prodrug Doxo-C-C-Fol was synthesized using the same protocol used for the synthesis of the activatable prodrug Doxo-S-S-Fol, but DSS was used as a cross-linker in place of DSP.

The synthesized probe was characterized by electrospray ionization mass spectrometry and HPLC showing the formation of highly pure noncleavable probe (Supporting Information Figure S2). The yield of the control prodrug Doxo-C-C-Fol was 75%. ESMS (ES + ve), (M<sup>+</sup>)<sub>calcd</sub> for C<sub>56</sub>H<sub>64</sub>N<sub>10</sub>O<sub>18</sub>: 1164.44, found 1163.96.

**In Situ Generation of Doxo-SH.** The aqueous solution of doxorubicin hydrochloride salt was added to PBS buffer solution (pH = 8.4) to obtain doxorubicin with free amine group. The resulting solution was centrifuged, and the solid pellet was soluble in DMSO. To this solution of doxorubicin (3.68 mM in DMSO), dithiobis(succinimidyl propionate) (DSP) solution (1.84 mM in DMSO) was added dropwise at room temperature. A catalytic amount of triethylamine (0.4  $\mu$ L in DMSO) was added to the reaction mixture. The progress of the reaction was monitored by TLC in 9:1 of chloroform and methanol. The reaction mixture was kept at room temperature for 30 min, before overnight incubation at 4 °C. The product (Doxo-S-S-Doxo) was then loaded on a silica gel column (flash column chromatography) to isolate the pure product using chloroform and methanol as eluant. A solution of DTT (1.84 mM in PBS, pH = 7.4) added to the product when Doxo-SH is required for an experiment.

**Fluorimetric Assessment of Activation of the Probes.** In these experiments, each probe (Doxo-S-S-Fol and Doxo-C-C-Fol) was incubated with a reducing agent (either GSH or DTT), and change in fluorescence emission ( $\lambda_{\text{ex}} = 497$  nm,  $\lambda_{\text{em}} = 594$  nm) was measured at designated time intervals using Horiba Jobin Yvon's Nanolog 3 fluorimeter. UV-vis spectra were recorded using a CARY 300 Bio UV-vis spectrophotometer.

**HPLC Experiment.** HPLC experiments were carried out using PerkinElmer's Series 200 instrument. In a typical experiment, upon addition of GSH to the disulfide probe (1:1 ratio), the release of Doxo-SH was monitored in a timely manner at 37 °C using HPLC chromatography.

**Cell Culture.** The human lung carcinoma (A549) and breast carcinoma (MCF 7) cells were maintained in accordance to the supplier's (ATCC) protocols. Briefly, the lung carcinoma cells were grown in a 5% FBS-containing Dulbecco's modified eagle medium (DMEM) supplemented with L-glutamine, streptomycin, amphotericin B, and sodium bicarbonate. The MCF 7 cells were propagated in a 10% FBS-containing minimum essential medium (MEM) containing penicillin, streptomycin, and bovine insulin (0.01 mg/mL). Cells were grown in a humidified incubator at 37 °C under 5% CO<sub>2</sub> atmosphere.

**Cytotoxicity Assay.** Corresponding cells (2500 cells/well) were seeded in 96-well plates, incubated with the corresponding probes (1.2  $\mu$ M) at 37 °C. At the end of the incubation period, each well was washed three times with 1X PBS and treated with 30  $\mu$ L of MTT (5  $\mu$ g/ $\mu$ L) for 2 h. The resulting formazan crystals were dissolved in acidic isopropanol (0.1 N of HCl), and the absorbance was recorded at 570 and 750 nm (background), using a Synergy  $\mu$ Quant microtiter plate reader (Biotek). Experiments were performed in triplicates. The percentage of cell survival as a function of drug/prodrug concentration was then plotted to determine the relative IC<sub>50</sub> value, which stands for the drug/prodrug concentration needed to prevent cell proliferation by 50%.

**Fluorimetric Assessment of Intracellular Activation of the Probes.** Corresponding cells were seeded to reach confluency in a Costar's black polystyrene 96-well microtiter plate. The cells were treated with either probe (1.2  $\mu$ M), and at designated time intervals, the cells were washed three times with 1X PBS. Subsequently, 1 mL of 1X PBS was added to each well and fluorescence emission acquisition using the TECAN's infinite M200 PRO fluorescence microtiter plate-reader.

**Fluorescence Microscopy.** Corresponding cells (10 000 cells in small dishes) were incubated with the each probe (1.2  $\mu$ M) in a humidified incubator (37 °C, 5% CO<sub>2</sub>). Subsequently, the cells were thoroughly washed three times with 1X PBS and fixed with 10% formalin solution, followed by nuclear staining with DAPI (obtained from

Invitrogen). Then, multiple fluorescence images were obtained using an Olympus IX71 fluorescence microscope equipped with a 40× objective.

**Flow Cytometry.** One-color flow cytometry was done to assess the fluorescence enhancement of our probes upon incubation with folate receptor-expressing A549 cells in a humidified incubator at 37 °C under 5% CO<sub>2</sub> atmosphere. Cells were seeded to reach confluency in Petri dishes and treated with either probe (1.2 μM), and at designated time intervals, the cells were harvested after trypsinization and centrifugation at 1000 rpm for 8 min. Subsequently, the cell pellets were resuspended in 1 mL of 1X PBS, and flow cytometry was done using a BD FACSCalibur flow cytometer from BD Biosciences.

## ■ ASSOCIATED CONTENT

**S Supporting Information.** Additional supporting documents and experimental results, including mass spectrometric results and HPLC chromatograms confirming the formation of probes, UV–vis spectra, experiment showing the stability of the probes in serum, GSH concentration-dependent reduction of the activatable Doxo–S–S–Fol prodrug, complete ref 38, in vitro cytotoxicity, and fluorescence microscopic results. This material is available free of charge via the Internet at <http://pubs.acs.org>.

## ■ AUTHOR INFORMATION

### Corresponding Author

[jmperez@ucf.edu](mailto:jmperez@ucf.edu)

## ■ ACKNOWLEDGMENT

This work was supported in part by NIH Grant GM084331 and UCF-NSTC Start Up Fund, all to J.M.P. We thank Dr. Hampton Sessions and Dr. Gregory P. Roth of the Sanford-Burnham Medical Research Institute, Orlando, Florida for assistance with HPLC and mass spectrometric experiments.

## ■ REFERENCES

- (1) Kim, K.; Lee, M.; Park, H.; Kim, J. H.; Kim, S.; Chung, H.; Choi, K.; Kim, I. S.; Seong, B. L.; Kwon, I. C. *J. Am. Chem. Soc.* **2006**, *128*, 3490–3491.
- (2) Santra, S.; Kaittanis, C.; Perez, J. M. *Langmuir* **2010**, *26*, 5364–5373.
- (3) Jayaprakash, S.; Wang, X.; Heston, W. D.; Kozikowski, A. P. *Chem. Med. Chem.* **2006**, *1*, 299–302.
- (4) Low, P. S.; Henne, W. A.; Doorneweerd, D. D. *Acc. Chem. Res.* **2008**, *41*, 120–129.
- (5) Wang, F.; Wang, Y. C.; Dou, S.; Xiong, M. H.; Sun, T. M.; Wang, J. *ACS Nano* **2011**, *5*, 3679–3692.
- (6) Weinstein, R.; Segal, E.; Satchi-Fainaro, R.; Shabat, D. *Chem. Commun.* **2010**, *46*, 553–555.
- (7) Beaudette, T. T.; Cohen, J. A.; Bachelder, E. M.; Broaders, K. E.; Cohen, J. L.; Engleman, E. G.; Frechet, J. M. J. *Am. Chem. Soc.* **2009**, *131*, 10360–10361.
- (8) Boonyarattanakalin, S.; Hu, J.; Dykstra-Rummel, S. A.; August, A.; Peterson, B. R. *J. Am. Chem. Soc.* **2007**, *129*, 268–269.
- (9) Nakagawa, O.; Ming, X.; Huang, L.; Juliano, R. L. *J. Am. Chem. Soc.* **2010**, *132*, 8848–8849.
- (10) Weitman, S. D.; Weinberg, A. G.; Coney, L. R.; Zurawski, V. R.; Jennings, D. S.; Kamen, B. A. *Cancer Res.* **1992**, *52*, 6708–6711.
- (11) Ross, J. F.; Chaudhuri, P. K.; Ratnam, M. *Cancer* **1994**, *73*, 2432–2443.
- (12) Weitman, S. D.; Lark, R. H.; Coney, L. R.; Fort, D. W.; Frasca, V.; Zurawski, V. R., Jr.; Kamen, B. A. *Cancer Res.* **1992**, *52*, 3396–3401.
- (13) Mattes, M. J.; Major, P. P.; Goldenberg, D. M.; Dion, A. S.; Hutter, R. V.; Klein, K. M. *Cancer Res.* **1990**, *50*, 880–884.
- (14) Low, P. S.; Antony, A. C. *Adv. Drug Delivery Rev.* **2004**, *56*, 1055–1058.
- (15) Salazar, M. D.; Ratnam, M. *Cancer Metastasis Rev.* **2007**, *26*, 141–152.
- (16) Leamon, C. P.; Low, P. S. *Proc. Natl. Acad. Sci. U.S.A.* **1991**, *88*, 5572–5576.
- (17) Henne, W. A.; Doorneweerd, D. D.; Hilgenbrink, A. R.; Kularatne, S. A.; Low, P. S. *Bioorg. Med. Chem. Lett.* **2006**, *16*, 5350–5355.
- (18) Lee, J. W.; Lu, J. Y.; Low, P. S.; Fuchs, P. L. *Bioorg. Med. Chem.* **2002**, *10*, 2397–2414.
- (19) Leamon, C. P.; Reddy, J. A.; Vlahov, I. R.; Kleindl, P. J.; Vetzal, M.; Westrick, E. *Bioconjug. Chem.* **2006**, *17*, 1226–1232.
- (20) Leamon, C. P.; Reddy, J. A.; Vlahov, I. R.; Vetzal, M.; Parker, N.; Nicoson, J. S.; Xu, L. C.; Westrick, E. *Bioconjug. Chem.* **2005**, *16*, 803–811.
- (21) Vlahov, I. R.; Santhapuram, H. K.; Kleindl, P. J.; Howard, S. J.; Stanford, K. M.; Leamon, C. P. *Bioorg. Med. Chem. Lett.* **2006**, *16*, 5093–5096.
- (22) Leamon, C. P.; Low, P. S. *J. Biol. Chem.* **1992**, *267*, 24966–24971.
- (23) Leamon, C. P.; Pastan, I.; Low, P. S. *J. Biol. Chem.* **1993**, *268*, 24847–24854.
- (24) Ogawa, M.; Kosaka, N.; Longmire, M. R.; Urano, Y.; Choyke, P. L.; Kobayashi, H. *Mol. Pharmaceutics* **2009**, *6*, 386–395.
- (25) Yang, J.; Chen, H.; Vlahov, I. R.; Cheng, J. X.; Low, P. S. *Proc. Natl. Acad. Sci. U.S.A.* **2006**, *103*, 13872–13877.
- (26) Urano, Y.; Asanuma, D.; Hama, Y.; Koyama, Y.; Barrett, T.; Kamiya, M.; Nagano, T.; Watanabe, T.; Hasegawa, A.; Choyke, P. L.; Kobayashi, H. *Nat. Med.* **2009**, *15*, 104–109.
- (27) Hilderbrand, S. A.; Weissleder, R. *Curr. Opin. Chem. Biol.* **2010**, *14*, 71–79.
- (28) McCarthy, J. R. *Adv. Drug Delivery Rev.* **2010**, *62*, 1023–1030.
- (29) Gounaris, E.; Tung, C. H.; Restaino, C.; Maehr, R.; Kohler, R.; Joyce, J. A.; Ploegh, H. L.; Barrett, T. A.; Weissleder, R.; Khazaei, K. *PLoS One* **2008**, *3*, e2916.
- (30) Elias, D. R.; Thorek, D. L.; Chen, A. K.; Czupryna, J.; Tsourkas, A. *Cancer Biomarkers* **2008**, *4*, 287–305.
- (31) Pham, W.; Pantazopoulos, P.; Moore, A. *J. Am. Chem. Soc.* **2006**, *128*, 11736–11737.
- (32) Xie, J.; Lee, S.; Chen, X. *Adv. Drug Delivery Rev.* **2010**, *62*, 1064–1079.
- (33) Olson, E. S.; Jiang, T.; Aguilera, T. A.; Nguyen, Q. T.; Ellies, L. G.; Scadeng, M.; Tsien, R. Y. *Proc. Natl. Acad. Sci. U.S.A.* **2010**, *107*, 4311–4316.
- (34) Rautio, J.; Kumpulainen, H.; Heimbach, T.; Oliyai, R.; Oh, D.; Jarvinen, T.; Savolainen, J. *Nat. Rev. Drug Discovery* **2008**, *7*, 255–270.
- (35) Gynther, M.; Laine, K.; Ropponen, J.; Leppanen, J.; Mannila, A.; Nevalainen, T.; Savolainen, J.; Jarvinen, T.; Rautio, J. *J. Med. Chem.* **2008**, *51*, 932–936.
- (36) Rodriguez, E.; Nilges, M.; Weissleder, R.; Chen, J. W. *J. Am. Chem. Soc.* **2010**, *132*, 168–177.
- (37) Han, H. K.; Amidon, G. L. *AAPS PharmSci.* **2000**, *2*, E6.
- (38) Jones, R. E.; et al. *Nat. Med.* **2000**, *6*, 1248–1252.
- (39) Huttunen, K. M.; Mahonen, N.; Raunio, H.; Rautio, J. *Curr. Med. Chem.* **2008**, *15*, 2346–2365.
- (40) Anbharasi, V.; Cao, N.; Feng, S.-S. *J. Biomed. Mater. Res.* **2010**, *94*, 730–743.
- (41) Santra, S.; Kaittanis, C.; Perez, J. M. *Mol. Pharmaceutics* **2010**, *7*, 1209–1222.
- (42) Garsky, V. M.; Lumma, P. K.; Feng, D. M.; Wai, J.; Ramjit, H. G.; Sardana, M. K.; Oliff, A.; Jones, R. E.; DeFeo-Jones, D.; Freidinger, R. M. *J. Med. Chem.* **2001**, *44*, 4216–4224.
- (43) Zou, P.; Yu, Y.; Wang, Y. A.; Zhong, Y.; Welton, A.; Galban, C.; Wang, S.; Sun, D. *Mol. Pharmaceutics* **2010**, *7*, 1974–1984.
- (44) Yoo, H. S.; Park, T. G. *J. Controlled Release* **2001**, *70*, 63–70.
- (45) Ducry, L.; Stump, B. *Bioconjug. Chem.* **2010**, *21*, 5–13.
- (46) Kaittanis, C.; Santra, S.; Perez, J. M. *J. Am. Chem. Soc.* **2009**, *131*, 12780–12791.

- (47) Yoon, S. A.; Choi, J. R.; Kim, J. O.; Shin, J. Y.; Zhang, X.; Kang, J. H. *Cancer Res. Treat.* **2010**, *42*, 163–171.
- (48) You, J.; Li, X.; de Cui, F.; Du, Y. Z.; Yuan, H.; Hu, F. Q. *Nanotechnology* **2008**, *19* (045102), 9pp.
- (49) Yuan, H.; Miao, J.; Du, Y. Z.; You, J.; Hu, F. Q.; Zeng, S. *Int. J. Pharm.* **2008**, *348*, 137–145.
- (50) Chung, K. N.; Saikawa, Y.; Paik, T. H.; Dixon, K. H.; Mulligan, T.; Cowan, K. H.; Elwood, P. C. *J. Clin. Invest.* **1993**, *91*, 1289–1294.
- (51) Yokochi, T.; Robertson, K. D. *Mol. Pharmacol.* **2004**, *66*, 1415–1420.
- (52) Riebeseel, K.; Biedermann, E.; Loser, R.; Breiter, N.; Hanselmann, R.; Mulhaupt, R.; Unger, C.; Kratz, F. *Bioconjug. Chem.* **2002**, *13*, 773–785.
- (53) Santra, S.; Kaittanis, C.; Grimm, J.; Perez, J. M. *Small* **2009**, *5*, 1862–1868.